2003 IEEE MTT-S Int. Microwave Symp. Dig., Philadelphia, PA, June 8-13, 2003, pp. 1507-1510. Presented by Kate Remley.

Sampling Oscilloscope Models and Calibrations

Kate A. Remley and Dylan F. Williams

National Institute of Standards and Technology, 325 Broadway, Boulder, CO 80305

***Abstract* — We discuss the basic principles of operation of electrical sampling oscilloscopes and describe circuit models developed to design, characterize, and help explain their operation. We survey common oscilloscope calibration schemes that correct for finite oscilloscope impulse response, distortion and jitter in the oscilloscope time base, and impedance mismatches.**

I. Introduction

We describe some electrical models of sampling circuits, some of which are of own invention. We show how these models complement each other, both for the design and characterization of sampling oscilloscopes, as well as for understanding their operation. We then turn to methods of calibrating sampling oscilloscopes, surveying schemes that characterize and correct for their impulse responses, which are of finite duration. We also briefly discuss calibrations that correct for imperfections and jitter in oscilloscope time bases and impedance mismatches in the measurements.

II. Sampling Oscilloscope Operation

Figure 1 contains a simplified schematic diagram of a two-diode sampling circuit. The bias supplies shown in the figure place the diodes in a high-impedance reverse-biased state except when the strobe fires. Each time the strobe fires, the strobe pulse turns the two diodes on, lowering their impedance for a short time. While the diodes are in their low-impedance on state, a nonzero voltage at the input port causes a net charge to flow from the input port through the diodes to the hold capacitors. This net injected charge is proportional to the voltage at the input port when the strobe was fired.

The balanced strobe configuration of the sampling circuit ensures that only the net charge transferred to the hold capacitors produces a signal at the output: differential charges transferred by the strobe pulses cancel. It is the sample of the signal at the output that is digitized and is proportional to the voltage at the input port when the strobe was fired.

In operation, a repetitive train of identical pulses is applied to the input port; the sampling circuit is used to reconstruct the shape of an individual pulse from the input pulse train. This is accomplished by firing the strobe during each repetition of the input pulse train at a time Δt later than it fired in the previous cycle of the input pulse train, as illustrated in Fig. 2. In this way the strobe firing time slowly "scans" across the input pulse being sampled. Since each successive digitized voltage sample corresponds to the input voltage at a short time Δt later than the previous voltage sample, the shape of the pulses in the input pulse train can be reconstructed from the digitized output voltage record.

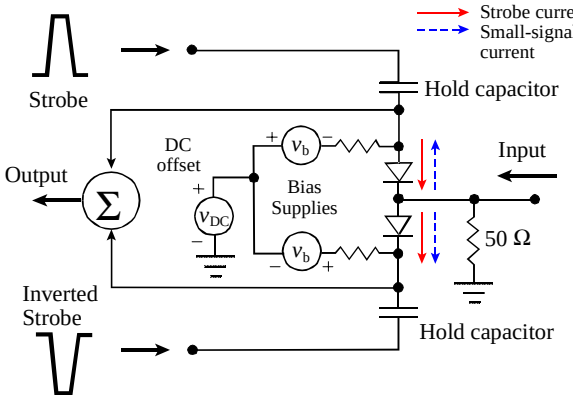

Fig. 1. Simplified electrical model of a sampling circuit.

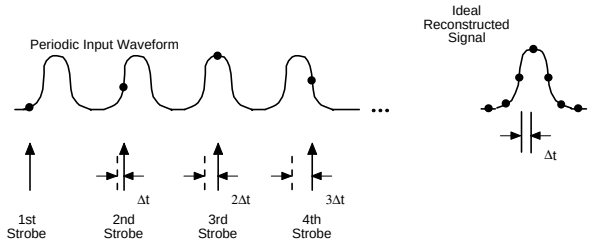

Fig. 2. Ideal sequential sampling and reconstruction.

III. Finite Duration of the Impulse Response

Figure 3 shows typical sampling-diode conductance and capacitance waveforms. If the diodes conducted only at the instant that the strobe was fired, the shape of the reconstructed signal at the output of the sampling circuit would exactly reproduce the shape of the individual pulses in the input pulse train.

However the strobe pulses and conductance waveform have a finite duration, and charge is injected on the hold capacitors in a nonuniform way over a finite time interval

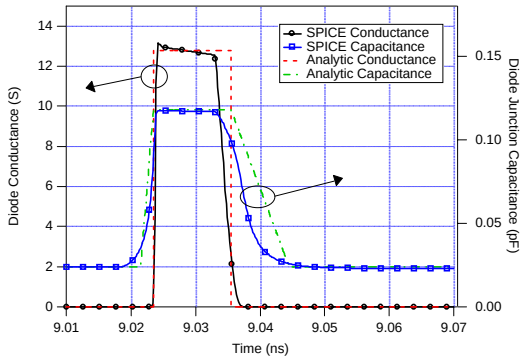

Fig. 3: Capacitance and conductance functions calculated from SPICE simulations (solid lines). The dashed lines show approximations of the capacitance and conductance functions. These were used in the analytic model of Ref. [9] to find the impulse response shown in Fig. 5.

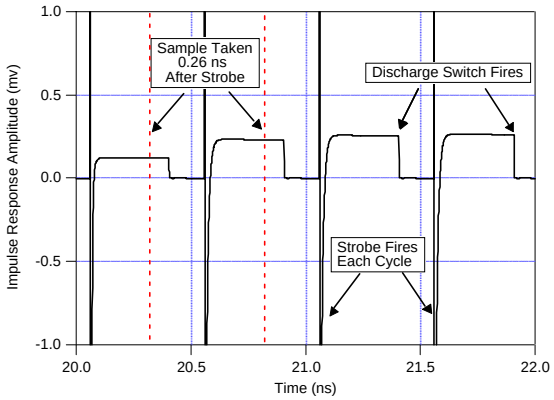

Fig. 4: A short segment of a SPICE simulation used to model the impulse response of a sampler. Each sampling cycle, the strobe fires, a voltage sample proportional to the impulse response is acquired (0.26 ns later), and then a switch discharges the hold capacitors.

that may be significantly longer than the sampling interval Δt. As a result, the nonideal response of the sampling circuit alters the reconstructed output. This phenomenon can be represented mathematically by convolving the input to the sampling circuit with the sampling circuit's "impulse response" [1]. Estimating impulse response is one useful application of oscilloscope models.

IV. SPICE Models

SPICE is a circuit simulator that uses large-signal, time-domain differential equations to solve for the voltages and currents in electrical circuits. Using SPICE, we can model an oscilloscope's behavior directly by modeling the sampling circuitry, including the strobe, sampling diodes, and hold capacitors.

To find the impulse response, we apply a repetitive train of short-duration input pulses (approximating Dirac delta functions) to the input of the sampling circuit [1-5]. SPICE simulations must be performed over enough sampling cycles to capture the entire impulse response, with a short enough time step to accurately represent rapidly changing signal features. This makes the calculations computationally intensive.

After each sample is acquired, the hold capacitor must discharge to its non-excited state, increasing the duration of the simulation. We use switches to discharge the hold capacitors and reduce simulation time [2-4]. This is illustrated in Fig. 4, where a small time segment of an impulse response simulation is shown. An alternate method uses one simulation for each time sample [5]. In either case, the impulse response must be reconstructed later from the calculated voltage on the hold capacitor with a post processor.

Calculating small-signal quantities such as junction capacitance and conductance from SPICE simulations is made difficult by the fact that SPICE provides only the total large-signal voltage across the diode and the total current through the diode. However, by inserting small voltages and observing the overall change in large-signal voltage and current, we can extract the conductance and capacitance functions for a given sampling circuit. These can then be used to model the small-signal behavior of the sampler. This is how we obtained the SPICE conductance and capacitance functions shown in Fig. 3.

V. Analytic Models

References [6-8] develop small-signal analytic models for sampling circuits with resistive diodes and fixed capacitances. In [9] we extended these analytic models to include nonlinear junction capacitance. The analytic models are based on direct solutions of the differential equations governing the small-signal sampling-circuit model. The solutions are based on simple circuit topologies and require restrictive approximations not needed in the SPICE models discussed in the last section. Thus, while the analytic solutions are computationally much more efficient, and provide great insight into sampler operation, the simplicity of the models we can treat this way makes it difficult to accruately characterize real sampling circuitry.

Figure 5 compares the impulse response predicted from the analytic model of [9] to that predicted by a SPICE model. The agreement is reasonable given that in [9] the conductance waveform must be rectangular and the capacitance waveform trapezoidal, as shown in Fig. 4.

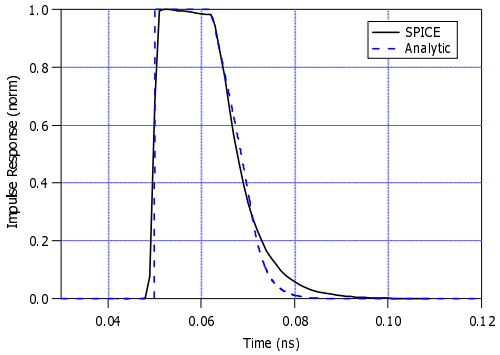

Fig. 5: Impulse response from a SPICE simulation [4] that utilizes an ideal trapezoidal strobe source (solid) and from the analytic model of [9] (dashed).

VI. Mixer Models

Microwave mixers and oscilloscope sampling circuits are based on the same principles of operation, and the distinction between the two is often blurred in actual instrumentation. Figure 6 illustrates the similarities. The mixer's local oscillator (LO) plays the role of the strobe in the oscilloscope, turning the mixer diodes on and off periodically. The mixer's high-frequency input (RF) corresponds to the oscilloscopes input signal, and the mixer intermediate-frequency (IF) output corresponds to the oscilloscope's sampled output.

The principle difference between the mixer and sampling circuit is that the strobe pulses used in sampling oscilloscopes are narrow and have many strong harmonics, whereas the mixer LO is a sinusoidal signal. In the sampling oscilloscope, it is the harmonics of the strobe pulses that mix directly with the nearest frequency components of the oscilloscope's input signal. On the other hand, in the mixer, it is the local oscillator's fundamental that mixes with the nearby RF frequencies.

Raleigh and Bellantoni used the similarity of mixers and samplers to development a resistive sampling-circuit model [10]. Diode conductance and capacitance calculations such as those of Fig. 3 can, at least in principle, be married with the classic mixer models of [11] and [12] to determine the frequency response of sampling circuits.

VII. Determining Oscilloscope Impulse Response Through Measurement

The impulse response of a sampling oscilloscope is easily determined from a measurement of a fast well-characterized pulse [13, 14]. However, there are also other ways of finding an oscilloscope's impulse response.

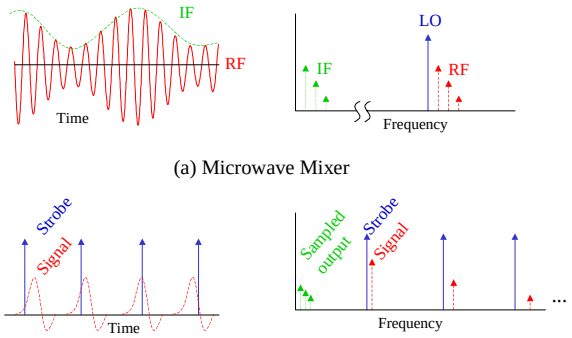

Fig. 6: Microwave-mixer/sampling-oscilloscope analogy.

A. Characterization of a Fast Pulse Source

The usual way of characterizing a pulse source later used for oscilloscope calibration involves constructing a much faster oscilloscope than the one you wish to characterize. In the past, national metrology laboratories have relied either on very fast electrical oscilloscopes [13, 14], sometimes based on superconducting electronics, or specialized oscilloscopes based on electro-optic interactions [15-18] to characterize fast pulse sources.

B. Swept-Sine Calibration

The swept-sine calibration [6] determines the magnitude of the frequency response of a sampling oscilloscope. The magnitude of the oscilloscope's frequency response is found by measuring sinusoids whose amplitudes have been determined with traceable microwave power measurements. However, the calibration is incomplete, as it does not determine the phase response of the oscilloscope.

C. Nose-to-Nose Calibration

Just over a decade ago, researchers at one of the digital oscilloscope manufacturing companies noticed that when a DC offset was applied to the hold capacitors in their oscilloscope, a short "kickout" pulse appeared at the input port. This pulse is almost identical in shape to the time-domain "impulse" response of the oscilloscope itself. When the input ports of two identical oscilloscopes of this type are connected together "nose-to-nose," the similarity of the kickout pulse and impulse response can be used to extract the response of one of the oscilloscopes. In practice, since no two oscilloscopes are truly identical, a series of measurements made with three oscilloscopes is required to extract the impulse response [6]. Knowledge of the oscilloscope's impulse response can subsequently be used to correct waveforms measured on the oscilloscope.

We have used the models of [1-4] and [9] to investigate the nose-to-nose assumption that the kickout pulse and impulse response of the oscilloscope are equal.

VIII. Time-Base Distortion and Jitter

After detecting a trigger pulse, the oscilloscope time base inserts a variable delay before firing the strobe. Systematic errors and distortion in this delay are referred to as time base distortion (TBD), and random noise in the delay circuit is referred to as jitter. Both TBD and jitter can be characterized by measuring a number of sinusoids of different phases and frequencies with the oscilloscope. The calibration methods then use the periodic properties of these input signals to characterize the oscilloscope's TBD and jitter [19].

IX. Mismatch Correction

High-frequency oscilloscopes are often designed to measure the voltage V_{50} a device will supply to an ideal 50 Ω load. However, the oscilloscope itself rarely has a perfect 50 Ω input impedance.

This impedance mismatch is often reduced in temporal calibrations by adding a precision air line to the front end of the oscilloscope: the overall system then has an impedance equal to the characteristic impedance of the airline, which is designed to be close to 50 Ω, over the time it takes for signals to perform a round trip in the airline. This gives a short time window over which the oscilloscope measures the convolution of V_{50} and the oscilloscope impulse response.

Frequency-domain methods allow mismatch-corrected measurements over longer time windows. These corrections are performed by measuring the impedances of the oscilloscope and the device under test with a vector network analyzer. These measured impedances can then used to calculate V_{50} from the voltage measured by the oscilloscope [20]. The time-base distortion corrections discussed in the previous section are required to accurately accomplish these frequency-domain mismatch corrections.

References

[1] D.F. Williams, K.A. Remley, and D.C. DeGroot, "Nose-to-nose response of a 20 GHz sampling circuit," *54th ARFTG Conf. Dig.*, pp. 64-70, Dec. 1999.

[2] K. A. Remley, D. F. Williams, and D. C. DeGroot, "Realistic Sampling-Circuit Model for a Nose-to-Nose Calibration," *IEEE MTT-S Int. Microwave Symp. Dig.*, pp. 1473-1476, June 2000.

[3] K. A. Remley, D. F. Williams, D. C. DeGroot, J. Verspecht, and J. Kerley, "Effects of nonlinear diode junction capacitance on the nose-to-nose calibration," *IEEE Microwave and Wireless Comp. Lett.*, vol. 11, pp. 196-198, May 2001.

[4] K. A. Remley, "The impact of internal sampling circuitry on the phase error inherent in the nose-to-nose oscilloscope calibration," *Natl. Inst. Stand. Technol. Tech. Note #1528*, submitted for publication 2002.

[5] J. Kerley, Agilent Technologies, Colorado Springs, CO, Private Communication, March 1991.

[6] J. Verspecht and K. Rush, "Individual characterization of broadband sampling oscilloscopes with a nose-to-nose calibration procedure," *IEEE Trans. Instrum. Meas.*, vol. 43, no. 2, pp. 347-354, April 1994.

[7] J. Verspecht, "Broadband sampling oscilloscope characterization with the 'nose-to-nose' calibration procedure: a theoretical and practical analysis," *IEEE Trans. Instrum. Meas.*, vol. 44, no. 6, pp. 991-997, December 1995.

[8] J. Verspecht, "Calibration of a Measurement System for High Frequency Nonlinear Devices," Ph.D. Thesis, Free University of Brussels, Brussels, Belgium, Sept. 1995.

[9] D.F. Williams and K.A. Remley, "Analytic sampling-circuit model," *IEEE Trans. Microwave Theory Tech.*, vol. 49, no. 6, pp. 1013-1019, June 2001.

[10] G.C. Raleigh and J.V. Bellantoni, "Determination of schottky diode sampling mixer frequency response from diode conductance waveforms," *IEEE Trans. Microwave Theory and Tech.*, vol. 41, no. 4, pp. 723-726, April 1993.

[11] H.C. Torrey and C.A. Whitmer, *Crystal Rectifiers*, New York: McGraw-Hill, 1948.

[12] S.A. Maas, *Microwave Mixers*, 2nd ed. Boston, MA: Artech House, 1993.

[13] W. L. Gans, "Dynamic calibration of waveform recorders and oscilloscopes using pulse standards," *IEEE Trans. Instrum. and Measurement*, vol. 39, pp. 952-957, Dec. 1990.

[14] J. P. Deyst, N. G. Paulter, T. Daboczi, G. N. Stenbakken, and T. M. Souders, "A fast-pulse oscilloscope calibration system," *IEEE Trans. Instrum. and Measurement*, vol. 47, pp. 1037-1041, Oct. 1998.

[15] D. Henderson and A.G. Roddie, "Calibration of fast sampling oscilloscopes," *Meas. Sci. Technol.*, vol. 1, pp. 673-679, 1990.

[16] D.F. Williams, P.D. Hale, T.S. Clement, and J.M. Morgan, "Mismatch corrections for electro-optic sampling systems," *56th ARFTG Conf. Dig.*, pp. 141-145, Nov. 30-Dec. 1, 2000.

[17] D.F. Williams, P.D. Hale, T.S. Clement, and J.M. Morgan, "Calibrating electro-optic sampling systems," *Int. Microwave Symp. Dig.*, Phoenix, AZ, pp. 1527-1530, May 20-25, 2001.

[18] T.S. Clement, P.D. Hale, D.F. Williams, and J.M. Morgan, "Calibrating photoreciever response to 110 GHz," *15th IEEE Lasers Electro-Optics Soc. Conf. Dig.*, Nov. 10-14, 2002, Glasglow, Scotland.

[19] P. D. Hale, T. S. Clement, K. J. Coakley, C. M. Wang, D. C. DeGroot, and A. P. Verdoni, "Estimating the magnitude and phase response of a 50 GHz sampling oscilloscope using the `Nose-to-Nose' method," *55th ARFTG Conf. Dig.*, June 2000.

[20] D.C. DeGroot, P.D. Hale, M. Vanden Bossche, F. Verbeyst, and J.Verspecht, "Analysis of interconnection networks and mismatch in the nose-to-nose calibration," *55th ARFTG Conf. Dig.*, June 2000.